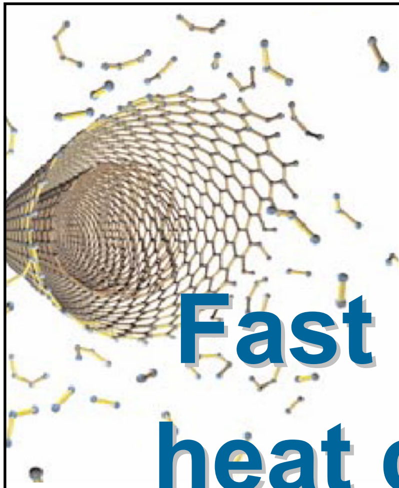

Fast Hybrid BNM Analysis of heat conduction properties of CNT-based composites

Masa. Tanaka, J. Zhang, M. Endo

Shinshu University
Faculty of Engineering

21st Symposium on Boundary Element Methods
第21回境界要素法シンポジウム

Background

- **Thermal conductivity of CNT (W/m·K)**

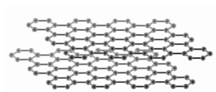

Graphite
50~100

Diamond
3320

Nanotube
3000~6000

Resins: 0~1 W/m·K

Metals: Fe 72 W/m·K
Cu 390 W/m·K

- **Promising applications**

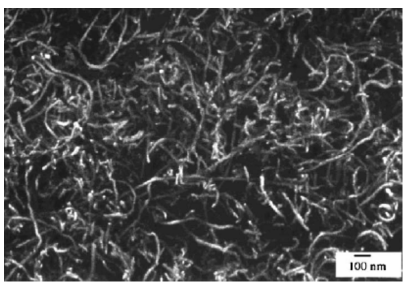

Nanotube-reinforced polymers

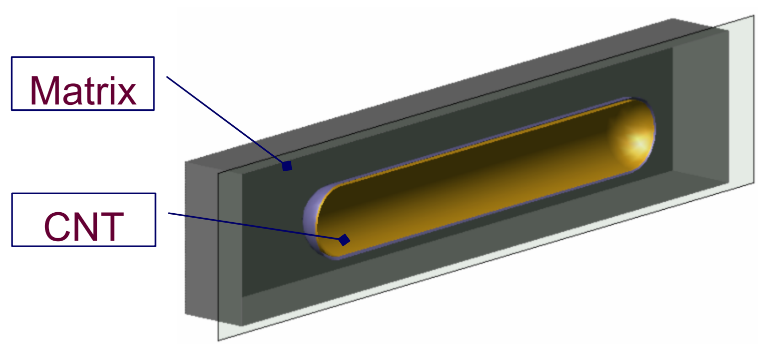

Representative Volume Element (RVE)

- **Objective of the research**

Standard numerical methods

◆ Mesh-based methods: FEM or BEM

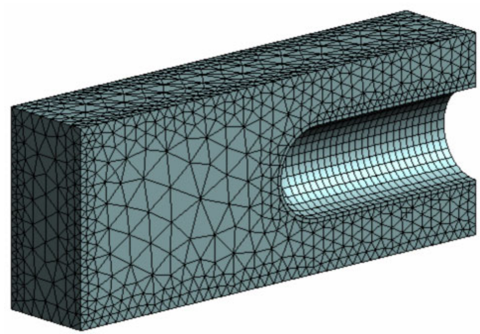

FEM/BEM Mesh

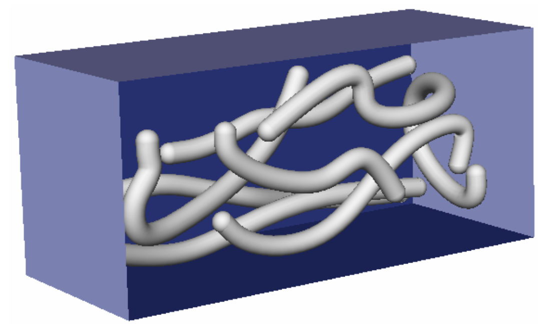

RVE including curved CNTs

Remarks:

- When an RVE including many randomly scattered CNTs, the high quality finite/boundary elements are difficult and cumbersome to obtain.
- Computational scale will become extremely large and the problem may be ill-conditioned due to the huge difference of heat conductivity between the CNT and polymer.

Hybrid BNM

Main features:

- Combines a modified functional with the *Moving Least Squares* (MLS) approximation
- Three independent variables
  - internal temperature
  - boundary temperature
  - boundary normal flux

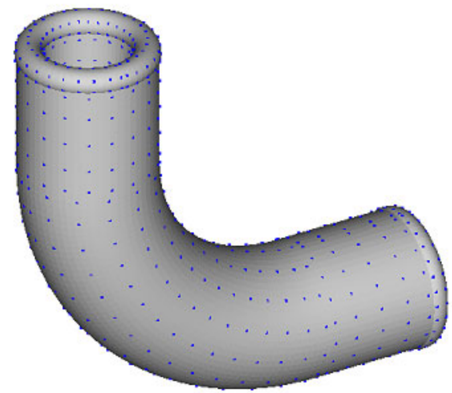

Example of meshless discretization

Variables approximation

- Domain variables

$$\phi = \sum_{I=1}^{N} \phi_I^s x_I \qquad \phi_I^s = \frac{1}{\kappa} \frac{1}{4\pi r(Q, \mathbf{s}_I)}$$

- Boundary variables

$$\tilde{\phi}(\mathbf{s}) = \sum_{I=1}^{N} \Phi_I(\mathbf{s}) \hat{\phi}_I \qquad \tilde{q}(\mathbf{s}) = \sum_{I=1}^{N} \Phi_I(\mathbf{s}) \hat{q}_I$$

Hybrid BNM (2)

- **System of equations**

$$\boxed{\mathbf{Ux} = \mathbf{H}\hat{\mathbf{q}}}$$

$$\boxed{\mathbf{Vx} = \mathbf{H}\hat{\phi}}$$

$$U_{IJ} = \int_{\Gamma_s^J} \phi_I^s v_J(Q)\, d\Gamma$$

$$V_{IJ} = \int_{\Gamma_s^J} q_I^s v_J(Q)\, d\Gamma$$

$$H_{IJ} = \int_{\Gamma_s^J} \Phi_I(\mathbf{s}) v_J(Q)\, d\Gamma$$

Remarks:

- **Noting that all integrations are performed in a local region without using any elements, the method is truely meshless.**

Simplified model

- **Hybrid BNM equations for Polymer matrix**

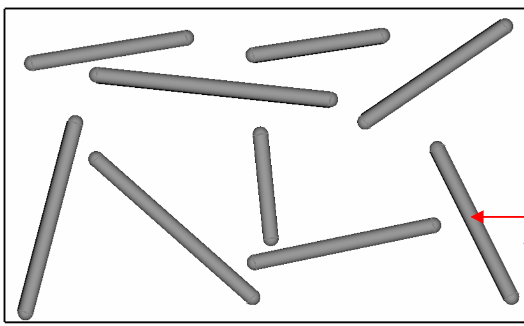

An RVE including n CNTs

$$\begin{bmatrix} \boldsymbol{U}_{00}^{p} & \boldsymbol{U}_{01}^{p} & \cdots & \boldsymbol{U}_{0n}^{p} \\ \boldsymbol{U}_{10}^{p} & \boldsymbol{U}_{11}^{p} & \cdots & \boldsymbol{U}_{1n}^{p} \\ \vdots & \vdots & \ddots & \vdots \\ \boldsymbol{U}_{n0}^{p} & \boldsymbol{U}_{n1}^{p} & \cdots & \boldsymbol{U}_{nn}^{p} \end{bmatrix} \begin{Bmatrix} \boldsymbol{x}_{0}^{p} \\ \boldsymbol{x}_{1}^{p} \\ \vdots \\ \boldsymbol{x}_{n}^{p} \end{Bmatrix} = \begin{Bmatrix} \boldsymbol{H}_{0}^{p}\hat{\boldsymbol{\phi}}_{0}^{p} \\ \boldsymbol{H}_{1}^{p}\hat{\boldsymbol{\phi}}_{1}^{p} \\ \vdots \\ \boldsymbol{H}_{n}^{p}\hat{\boldsymbol{\phi}}_{n}^{p} \end{Bmatrix}$$

$$\begin{bmatrix} \boxed{\boldsymbol{V}_{00}^{p}} & \boxed{\boldsymbol{V}_{01}^{p}} & \cdots & \boldsymbol{V}_{0n}^{p} \\ \boldsymbol{V}_{10}^{p} & \boldsymbol{V}_{11}^{p} & \cdots & \boldsymbol{V}_{1n}^{p} \\ \vdots & \vdots & \ddots & \vdots \\ \boldsymbol{V}_{n0}^{p} & \boldsymbol{V}_{n1}^{p} & \cdots & \boldsymbol{V}_{nn}^{p} \end{bmatrix} \begin{Bmatrix} \boldsymbol{x}_{0}^{p} \\ \boldsymbol{x}_{1}^{p} \\ \vdots \\ \boldsymbol{x}_{n}^{p} \end{Bmatrix} = \begin{Bmatrix} \boldsymbol{H}_{0}^{p}\hat{\boldsymbol{q}}_{0}^{p} \\ \boldsymbol{H}_{1}^{p}\hat{\boldsymbol{q}}_{1}^{p} \\ \vdots \\ \boldsymbol{H}_{n}^{p}\hat{\boldsymbol{q}}_{n}^{p} \end{Bmatrix}$$

Simplified model (2)

- **Assembled equation for polymer domain**

$$\begin{bmatrix} U_{00}^p & U_{01}^p & \cdots & U_{0n}^p \\ U_{10}^p & U_{11}^p & \cdots & U_{1n}^p \\ \vdots & \vdots & \ddots & \vdots \\ U_{n0}^p & U_{n1}^p & \cdots & U_{nn}^p \end{bmatrix} \begin{Bmatrix} x_0^p \\ x_1^p \\ \vdots \\ x_n^p \end{Bmatrix} = \begin{Bmatrix} H_0^p \hat{\phi}_0^p \\ H_1^p \hat{\phi}_1^p \\ \vdots \\ H_n^p \hat{\phi}_n^p \end{Bmatrix}$$

$$\begin{bmatrix} V_{00}^p & V_{01}^p & \cdots & V_{0n}^p \\ V_{10}^p & V_{11}^p & \cdots & V_{1n}^p \\ \vdots & \vdots & \ddots & \vdots \\ V_{n0}^p & V_{n1}^p & \cdots & V_{nn}^p \end{bmatrix} \begin{Bmatrix} x_0^p \\ x_1^p \\ \vdots \\ x_n^p \end{Bmatrix} = \begin{Bmatrix} H_0^p \hat{q}_0^p \\ H_1^p \hat{q}_1^p \\ \vdots \\ H_n^p \hat{q}_n^p \end{Bmatrix}$$

$$\Rightarrow \begin{bmatrix} A_{00} & A_{01} & \cdots & A_{0n} \\ U_{10} & U_{11} & \cdots & U_{1n} \\ \vdots & \vdots & \ddots & \vdots \\ U_{n0} & U_{n1} & \cdots & U_{nn} \end{bmatrix} \begin{Bmatrix} x_0 \\ x_1 \\ \vdots \\ x_n \end{Bmatrix} = \begin{Bmatrix} H_0 d_0 \\ H_1 \hat{\phi}_1 \\ \vdots \\ H_n \hat{\phi}_n \end{Bmatrix}$$

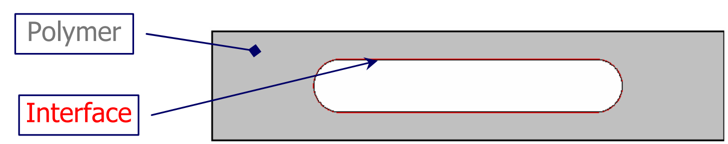

- **Constant temperature at interfaces**

$$\{\phi_k\} = \{\mathbf{1}\}_k \phi_c^k$$

Simplified model (3)

- **Equation with constraint**

$$\begin{bmatrix} \boldsymbol{A}_{00} & \boldsymbol{A}_{01} & \cdots & \boldsymbol{A}_{0n} & \mathbf{0} & \cdots & \mathbf{0} \\ \boldsymbol{U}_{10} & \boldsymbol{U}_{11} & \cdots & \boldsymbol{U}_{1n} & \boldsymbol{H}_1\{\mathbf{1}\}_1 & \cdots & \mathbf{0} \\ \vdots & \vdots & \ddots & \vdots & \vdots & \ddots & \vdots \\ \boldsymbol{U}_{n0} & \boldsymbol{U}_{n1} & \cdots & \boldsymbol{U}_{nn} & \mathbf{0} & \cdots & \boldsymbol{H}_n\{\mathbf{1}\}_n \end{bmatrix} \begin{Bmatrix} \boldsymbol{x}_0 \\ \boldsymbol{x}_1 \\ \vdots \\ \boldsymbol{x}_n \\ \phi_c^1 \\ \vdots \\ \phi_c^n \end{Bmatrix} = \begin{Bmatrix} \boldsymbol{H}_0 \boldsymbol{d}_0 \\ \mathbf{0} \\ \vdots \\ \mathbf{0} \end{Bmatrix}$$

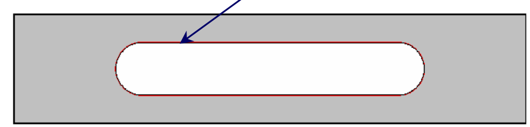

- **Additional equations**

$$\int_{C_k} q \, d\Gamma = 0$$

$$q = \sum_{I=1}^{N} \frac{\partial \phi_I^s}{\partial n} x_I$$

$$\Rightarrow \quad \sum_{I=1}^{N} \int_{C_k} \frac{\partial \phi_I^s}{\partial n} d\Gamma x_I = 0$$

$$\int_{C_k} \frac{\partial \phi_I^s}{\partial n} d\Gamma = \begin{cases} 1, & \forall \mathbf{s}_I \in C_k \\ 0, & \forall \mathbf{s}_I \notin C_k \end{cases}$$

$$\Rightarrow \quad \{\mathbf{1}\}^{\mathrm{T}} \{\boldsymbol{x}_k\} = 0$$

Simplified model (4)

- **Final system of equations**

$$\begin{bmatrix} \boldsymbol{A}_{00}^0 & \boldsymbol{A}_{01}^0 & \cdots & \boldsymbol{A}_{0n}^0 & \mathbf{0} & \cdots & \mathbf{0} \\ \boldsymbol{U}_{10}^0 & \boldsymbol{U}_{11}^0 & \cdots & \boldsymbol{U}_{1n}^0 & \boldsymbol{H}_1\{\mathbf{1}\}_1 & \cdots & \mathbf{0} \\ \mathbf{0} & \{\mathbf{1}\}_1^{\mathrm{T}} & \cdots & \mathbf{0} & 0 & \cdots & 0 \\ \vdots & \vdots & \ddots & \vdots & \vdots & \ddots & \vdots \\ \boldsymbol{U}_{n0}^0 & \boldsymbol{U}_{n1}^0 & \cdots & \boldsymbol{U}_{nn}^0 & \mathbf{0} & \cdots & \boldsymbol{H}_n\{\mathbf{1}\}_n \\ \mathbf{0} & \mathbf{0} & \cdots & \{\mathbf{1}\}_n^{\mathrm{T}} & 0 & \cdots & 0 \end{bmatrix} \begin{Bmatrix} \boldsymbol{x}_0 \\ \boldsymbol{x}_1 \\ \vdots \\ \boldsymbol{x}_n \\ \phi_c^1 \\ \vdots \\ \phi_c^n \end{Bmatrix} = \begin{Bmatrix} \boldsymbol{H}_0\boldsymbol{d}_0 \\ \mathbf{0} \\ 0 \\ \vdots \\ \mathbf{0} \\ 0 \end{Bmatrix}$$

Remarks: The product of a row of the coefficient matrix and a guess vector can be expressed as one of the following four sums:

$$\sum_{J=1}^{N} \int_{\Gamma_I} \phi_J^s v_I(Q) x_J \, d\Gamma \qquad \sum_{J=1}^{N} \int_{\Gamma_I} \phi_J^s v_I(Q) x_J \, d\Gamma + \phi_c^k \sum_{J}^{m_k} H_{IJ}$$

$$\sum_{J=1}^{N} \int_{\Gamma_I} -\kappa \frac{\partial \phi_J^s}{\partial n} v_I(Q) x_J \, d\Gamma \qquad \sum_{J}^{m_k} x_J^k$$

Accelerate Hybrid BNM with FMM

- **A hierarchy of boxes which refine the computational domain into small regions**

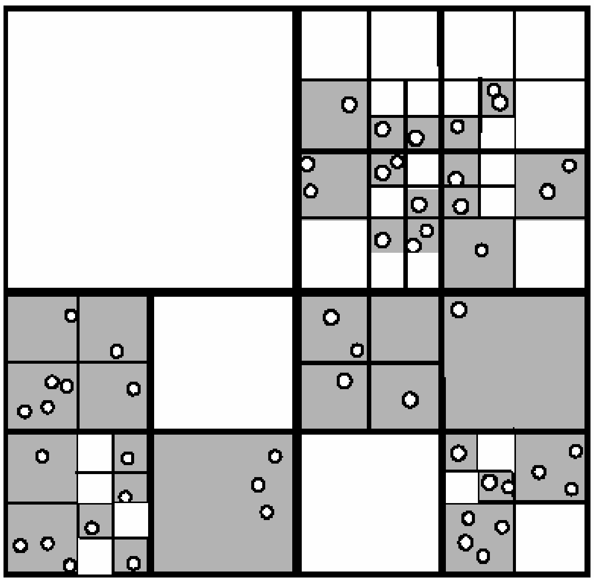

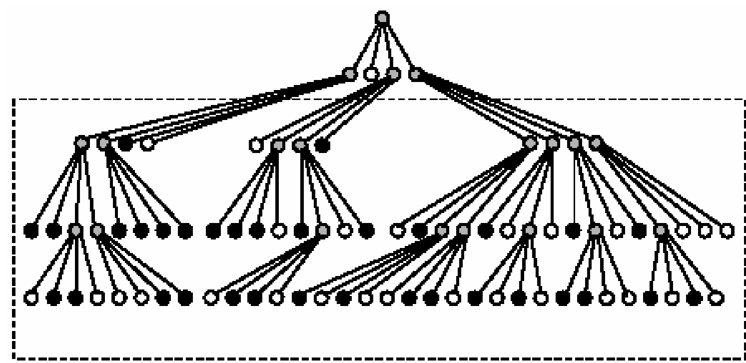

Quad-tree in 2D
Oct-tree in 3D

For simplicity, taking 2D case as an example.

Accelerate Hybrid BNM with FMM (2)

➤ **Multipole expansion**

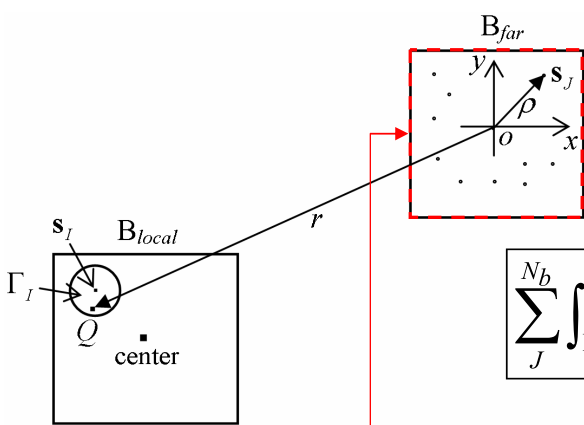

$$u_J^s = \frac{1}{4\pi}\frac{1}{r(Q,\mathbf{s}_J)} = \frac{1}{4\pi}\sum_{n=0}^{\infty}\sum_{m=-n}^{n}\rho^n Y_n^{-m}(\alpha,\beta)\frac{Y_n^m(\theta,\phi)}{r^{n+1}}$$

$$\boxed{\sum_J^{N_b}\int_{\Gamma_I} u_J^s v_I(Q) x_J d\Gamma = \frac{1}{4\pi}\sum_{n=0}^{\infty}\sum_{m=-n}^{n} M_n^m \int_{\Gamma_I}\frac{Y_n^m(\theta,\phi)}{r^{n+1}} v_I(Q) d\Gamma}$$

$$M_n^m = \sum_J^{N_b}\rho_J^n Y_n^{-m}(\alpha_J,\beta_J)x_J$$

Condition: $r > \rho$

In above expanded expression, the pair of points Q and $\mathbf{s}_J$ is separated.

Accelerate Hybrid BNM with FMM (3)

- **Local expansion**

$$\frac{Y_n^m(\theta,\phi)}{r^{n+1}} = \sum_{j=0}^{\infty}\sum_{k=-j}^{j} \frac{i^{|k-m|-|k|-|m|} A_n^m A_j^k Y_{n+j}^{m-k}(\alpha',\beta')}{(-1)^n A_{n+j}^{m-k} \rho'^{\,j+n+1}} Y_j^k(\theta',\phi') r'^{\,j}$$

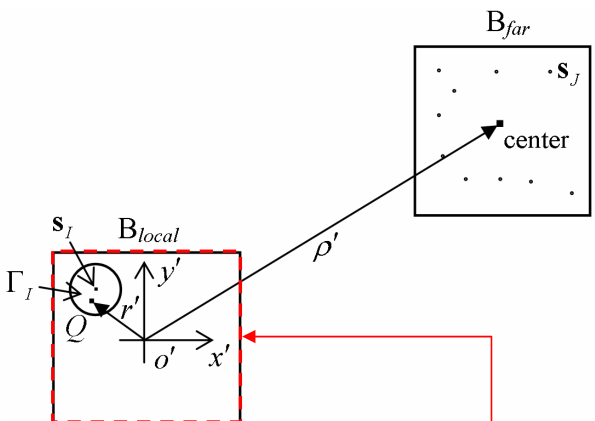

$$\boxed{\sum_{J}^{N_b} \int_{\Gamma_I} u_J^s v_I(Q) x_J d\Gamma = \sum_{j=0}^{\infty}\sum_{k=-j}^{j} L_j^k S_j^k}$$

$$\boxed{L_j^k = \sum_{J}^{N_b} \frac{Y_j^{-k}(\alpha_J,\beta_J)}{\rho_J'^{\,j+1}} x_J}$$

$$S_j^k = \frac{1}{4\pi}\int_{\Gamma_I} Y_j^k(\theta',\phi') r'^{\,j} v_I(Q) d\Gamma$$

Condition: $\rho' > 2r'$

Accelerate Hybrid BNM with FMM (4)

- **Translation operators**

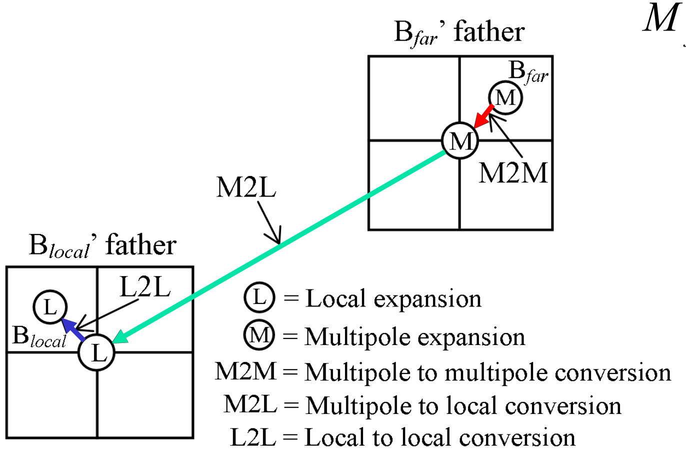

$$M'^{k}_{j} = \sum_{n=0}^{j} \sum_{m=-n}^{n} M^{k-m}_{j-n} \boxed{\frac{i^{|k|-|m|-|k-m|} A^{m}_{n} A^{k-m}_{j-n} \rho^{n} Y^{-m}_{n}(\alpha,\beta)}{A^{k}_{j}}}$$

multipole to multipole conversion

$$L^{k}_{j} = \sum_{n=0}^{\infty} \sum_{m=-n}^{n} M^{m}_{n} \boxed{\frac{i^{|k-m|-|k|-|m|} A^{m}_{n} A^{k}_{j} Y^{m-k}_{n+j}(\alpha',\beta')}{(-1)^{n} A^{m-k}_{n+j} \rho'^{\,j+n+1}}}$$

multipole to local conversion

$$L^{k}_{j} = \sum_{n=j}^{\infty} \sum_{m=-n}^{n} L'^{m}_{n} \boxed{\frac{i^{|m|-|m-k|-|k|} A^{m-k}_{n-j} A^{k}_{j} Y^{m-k}_{n-j}(\alpha,\beta) \rho^{n-j}}{(-1)^{n+j} A^{m}_{n}}}$$

local to local conversion

Accelerate Hybrid BNM with FMM (5)

- **Upward pass and Downward pass**

In FMM, the multipole and local moments are orchestrated in a hierarchy of boxes.

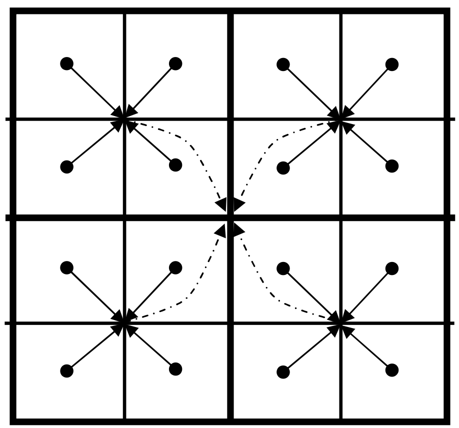

Level $l+1$ Level l

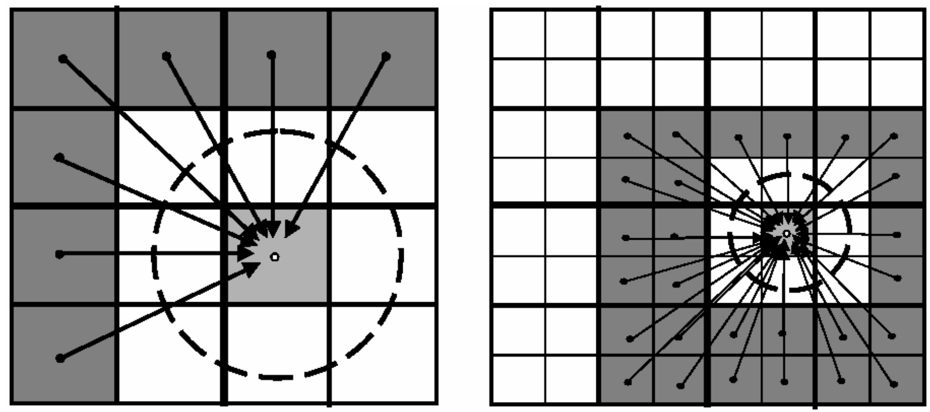

Level l Level $l+1$

Multipole moments are accumulated from leaves to the root (***Upward pass***); and local moments are distributed from the root to the leaves (***Downward pass***). This is accomplished in order of N operations.

Study on CNT alignment

- **RVE containing a number of CNTs**

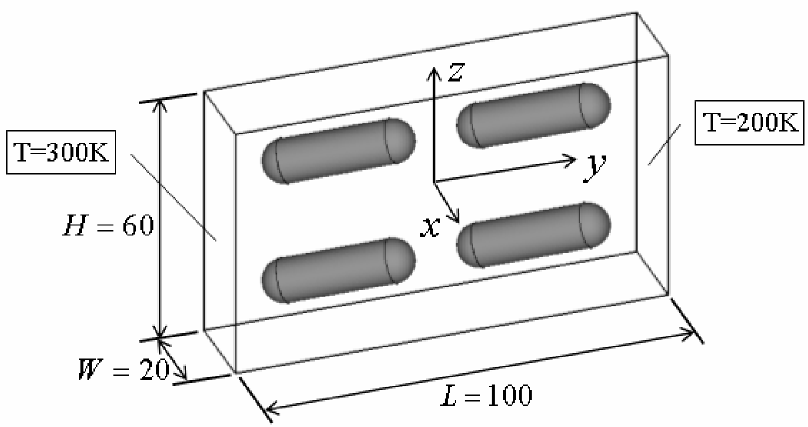

Dimensions (nm) *and Boundary condition of RVE*

Heat conductivity used for polymer: 0.37 W/m·K

$$\kappa = -\frac{qL}{\Delta T}$$

Equivalent heat conductivity

We will consider different lengths, numbers and alignments of CNTs in the RVE.

Study on CNT alignment (2)

- **Results obtained by direct solver**
  - **Four short CNTs**

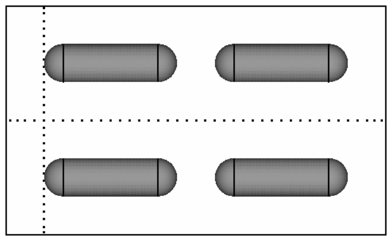
(a)

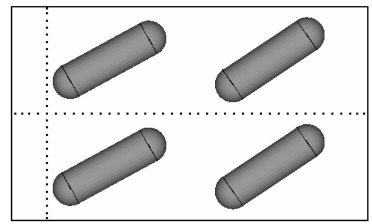
(b)

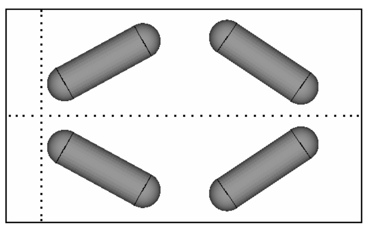
(c)

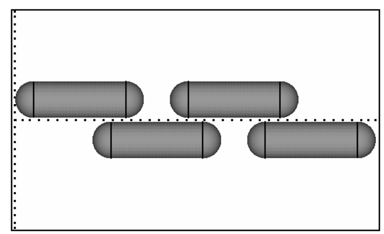
(d)

CNT alignments	(a)	(b)	(c)	(d)
Conductivity (W/m·K)	0.6974	0.5993	0.6015	0.9736

Study on CNT alignment (4)

- **Results obtained by FM-HBNM**
  - **Straight CNTs, alignment 1**

(a) (b) (c) (d) (e)

RVE	(a)	(b)	(c)	(d)	(e)
Volume percentage of CNT, v	3.136%	6.272%	9.408%	15.68%	21.95%
Equivalent conductivity, κ (W/m·K)	1.646	2.890	3.780	5.079	6.114
Increase of conductivity (times)	3.5	6.8	9.2	12.7	15.5
Effectiveness of enhancement κ/v	52.49	46.08	40.18	32.39	27.85

Study on CNT alignment (5)

- **Results obtained by FM-HBNM**
  - **Straight CNTs, alignment 2**

(a) (b) (c) (d) (e)

RVE	(a)	(b)	(c)	(d)	(e)
Volume percentage of CNT, r	6.381%	9.108%	11.84%	17.29%	22.74%
Equivalent conductivity, κ (W/m·K)	1.334	1.770	2.294	2.868	3.138
Increase of conductivity (times)	2.6	3.8	5.2	6.6	7.5
Effectiveness of enhancement κ/v	20.91	19.43	19.37	16.59	13.80

Study on CNT alignment (6)

- Results obtained by FM-HBNM
  - Curved CNTs

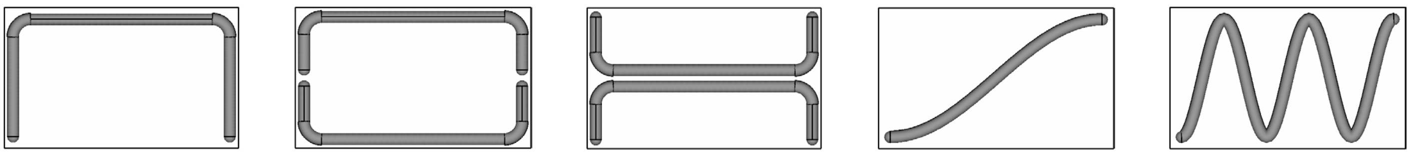

(a) (b) (c) (d) (e)

RVE	(a)	(b)	(c)	(d)	(e)
Volume percentage of CNT, r	6.198%	8.796%	8.796%	3.553%	9.010%
Equivalent conductivity, κ (W/m·K)	7.680	7.155	7.179	1.244	1.941
Increase of conductivity (times)	20	18	18	2.4	4.2
Effectiveness of enhancement κ/v	123.9	81.34	81.62	35.02	21.54

Conclusions

- A simplified mathematic model is proposed for simulation of thermal behavior of CNT-based composites. This model provides remarkable improvement in computational efficiency.
- The FMM has been successfully applied to speed the equation-solution process in the Hybrid BNM combined with the simplified model.
- Advanced computations have been performed for an RVE with long, straight/curved CNTs embedded. Some specific alignments were found that significantly increase the equivalent heat conductivity of the composite.